2990 *Inorg. Chem.* **2010**, *49*, 2990–2995
DOI: 10.1021/ic902493r

Inorganic Chemistry
Article

Lone Pairs as Chemical Scissors in New Antimony Oxychlorides, $Sb_2ZnO_3Cl_2$ and $Sb_{16}Cd_8O_{25}Cl_{14}$

Vinna Jo, Min Kyung Kim, Dong Woo Lee, Il-Wun Shim, and Kang Min Ok*

Department of Chemistry, Chung-Ang University, 221 Heukseok-dong, Dongjak-gu, Seoul 156-756, Korea

Received December 16, 2009

Two new metal antimony oxychlorides, $Sb_2ZnO_3Cl_2$ and $Sb_{16}Cd_8O_{25}Cl_{14}$, have been synthesized by solid-state reactions using Sb_2O_3 and $ZnCl_2$ (or $CdCl_2$) as reagents. The structures of $Sb_2ZnO_3Cl_2$ and $Sb_{16}Cd_8O_{25}Cl_{14}$ have been determined by single-crystal X-ray diffraction. Both of the reported materials contain Sb^{3+} cations that are in an asymmetric coordination environment attributable to their stereoactive lone pair. $Sb_2ZnO_3Cl_2$ has a novel two-dimensional layered structure consisting of distorted ZnO_2Cl_2 tetrahedra and SbO_3 polyhedra. $Sb_{16}Cd_8O_{25}Cl_{14}$ exhibits a one-dimensional structure consisting of Sb^{3+}−Cd^{2+}−oxide rods, Cd^{2+}−chloride double chains, and isolated Cl^- ions. Complete separation of the halophile and chalcophile moieties is observed from the reported materials. Detailed structural analysis, IR spectra, thermogravimetric analysis, ion-exchange reactions, and dipole moment calculations are presented. Crystal data: $Sb_2ZnO_3Cl_2$, orthorhombic, space group *Pnma* (No. 62), a = 17.124(4) Å, b = 5.5598(12) Å, c = 6.4823(14) Å, V = 617.2(2) Å^3, and Z = 4; $Sb_{16}Cd_8O_{25}Cl_{14}$, monoclinic, space group *I*2/*m* (No. 12), a = 14.251(3) Å, b = 3.9895(8) Å, c = 21.145(4) Å, β = 97.35(3)°, V = 1192.3(4) Å^3, and Z = 8.

Introduction

Materials containing lone-pair cations (i.e., Pb^{2+}, Sb^{3+}, Te^{4+}, I^{5+}, etc.) have drawn great attention, attributable to their specific functional properties such as second-harmonic generation, piezoelectricity, pyroelectricity, and ferroelectricity.[1−4] These technologically important material properties are certainly related to crystallographic noncentrosymmetry, which can be produced with ease from the inherent asymmetric coordination environment of stereoactive nonbonded electron pairs.[5−7] The lone pairs are considered to be the result of a second-order Jahn−Teller distortion,[8−12] which reduces the energy between the highest occupied (HOMO) s orbital and the lowest unoccupied (LUMO) p orbital through s−p mixing.[13−16] Also, materials with lone-pair cations have exhibited a rich structural chemistry in that they can adopt a variable coordination environment.[17,18] A great deal of interesting framework architecture is expected if the variable geometry of the lone-pair cations is further combined with polyhedra of transition-metal cations and halides. The combination, however, often resulted in low-dimensional materials with chains or layers. While the more chalcophilic lone-pair cations tend to make bonds with oxygen, the late transition metals are rather coordinated to halogen.[19−21] This kind of complete separation of the halophile and chalcophile substructures, in turn, forces the overall structures of the materials to form low dimensions such as chains or layers. Thus, both of the lone-pair cations and the halogen ions are often called "chemical scissors".[20,22−25] We have been very interested in investigating materials in the

*To whom correspondence should be addressed. E-mail: kmok@cau.ac.kr.

(1) Jona, F.; Shirane, G. *Ferroelectric Crystals*; Pergamon Press: Oxford, U.K., 1962.
(2) Cady, W. G. *Piezoelectricity; an Introduction to the Theory and Applications of Electromechanical Phenomena in Crystals*; Dover: New York, 1964.
(3) Lang, S. B. *Sourcebook of Pyroelectricity*; Gordon & Breach Science: London, 1974.
(4) Lines, M. E.; Glass, A. M. *Principles and Applications of Ferroelectrics and Related Materials*; Oxford University Press: Oxford, U.K., 1991.
(5) Gillespie, R. J.; Nyholm, R. S. *Q. Rev., Chem. Soc.* **1957**, *11*, 339.
(6) Orgel, L. E. *J. Chem. Soc.* **1959**, 3815.
(7) Seshadri, R.; Hill, N. A. *Chem. Mater.* **2001**, *13*, 2892.
(8) Opik, U.; Pryce, M. H. L. *Proc. R. Soc. London* **1957**, *A238*, 425.
(9) Bader, R. F. W. *Mol. Phys.* **1960**, *3*, 137.
(10) Bader, R. F. W. *Can. J. Chem.* **1962**, *40*, 1164.
(11) Pearson, R. G. *THEOCHEM* **1983**, *103*, 25.
(12) Wheeler, R. A.; Whangbo, M.-H.; Hughbanks, T.; Hoffmann, R.; Burdett, J. K.; Albright, T. A. *J. Am. Chem. Soc.* **1986**, *108*, 2222.
(13) Nikol, H.; Vogler, A. *J. Am. Chem. Soc.* **1991**, *113*, 8988.
(14) Nikol, H.; Vogler, A. *Inorg. Chem.* **1993**, *32*, 1072.
(15) Watson, G. W.; Parker, S. C. *J. Phys. Chem. B* **1999**, *103*, 1258.
(16) Watson, G. W.; Parker, S. C.; Kresse, G. *Phys. Rev. B* **1999**, *59*, 8481.
(17) Wickleder, M. S. *Chem. Rev.* **2002**, *102*, 2011.
(18) Ok, K. M.; Halasyamani, P. S. *Angew. Chem., Int. Ed.* **2004**, *43*, 5489.
(19) Semenova, T. F.; Rozhdestvenskaya, I. V.; Filatov, S. K.; Vergasova, L. P. *Miner. Mag.* **1992**, *56*, 241.
(20) Becker, R.; Johnsson, M.; Kremer, R. K.; Lemmens, P. *Solid State Sci.* **2003**, *5*, 1411.
(21) Mayerová, Z.; Johnsson, M.; Lidin, S. *J. Solid State Chem.* **2005**, *178*, 3471.
(22) Johnsson, M.; Tornroos, K. W.; Mila, F.; Millet, P. *Chem. Mater.* **2000**, *12*, 2853.
(23) Millet, P.; Bastide, B.; Pashchenko, V.; Gnatchenko, S.; Gapon, V.; Ksari, Y.; Stepanov, A. *J. Mater. Chem.* **2001**, *11*, 1152.
(24) Millet, P.; Johnsson, M.; Pashchenko, V.; Ksari, Y.; Stepanov, A.; Mila, F. *Solid State Ionics* **2001**, *141*, 559.

Published on Web 02/11/2010

metal−Sb^{3+}−oxychloride system. With respect to metal antimony oxychlorides, several materials have been reported, namely, $CuSbTeO_3Cl_2$,[20] $CuSb_2O_3Cl$,[21] $Cu_{20}Sb_{35}O_{44}Cl_{37}$,[25] $Hg_{12}SbO_6BrCl_2$,[26] $BaSbO_2Cl$,[27] $PbSbO_2Cl$,[28] and Sb_3TeO_6Cl.[29] Although the materials exhibit low-dimensional structures as expected, most reported materials show interesting structural features and/or material properties. For example, $Cu_{20}Sb_{35}O_{44}Cl_{37}$ consists of infinite chains of $[Cu_{10}Cl_{16}]^{6-}$ T3 supertetrahedra and isolated $[Sb_{35}Cl_5O_{44}]^{12+}$ clusters. Magnetic properties and conductivity have been measured on the layered $CuSbTeO_3Cl_2$. In this paper, we report the detailed structural analysis, IR spectra, thermogravimetric analysis (TGA), ion-exchange reactions, and dipole moment calculations of two new antimony oxychloride materials, $Sb_2ZnO_3Cl_2$ and $Sb_{16}Cd_8O_{25}Cl_{14}$. To the best of our knowledge, the materials are the first examples of Sb^{3+}−Zn^{2+}−O−Cl and Sb^{3+}−Cd^{2+}−O−Cl combinations. We also present how the lone pairs separate completely the halophile and chalcophile moieties for both materials.

Experimental Section

Syntheses. Sb_2O_3 (Alfa, 99.6%), $ZnCl_2$ (Aldrich, 98%), and $CdCl_2$ (Aldrich, 98%) were used as received. $Sb_2ZnO_3Cl_2$ and $Sb_{16}Cd_8O_{25}Cl_{14}$ were synthesized by standard solid-state reaction methods. For $Sb_2ZnO_3Cl_2$, 0.875 g (3.00×10^{-3} mol) of Sb_2O_3 and 0.409 g (3.00×10^{-3} mol) of $ZnCl_2$ were combined under an atmosphere of dry argon. For $Sb_{16}Cd_8O_{25}Cl_{14}$, 0.787 g (2.70×10^{-3} mol) of Sb_2O_3 and 0.495 g (2.70×10^{-3} mol) of $CdCl_2$ were combined under an atmosphere of dry argon. The respective mixtures were thoroughly mixed with an agate mortar and pestle and subsequently introduced into fused silica tubes and evacuated. Each tube sealed under vacuum was gradually heated to 250 °C for 5 h and then to 350 °C for 24 h (or 600 °C for 48 h for $Sb_{16}Cd_8O_{25}Cl_{14}$). The tubes were cooled to room temperature at a rate of 1 °C min^{-1}. The products contained colorless rod crystals and light-gray powder. The powder X-ray diffraction (XRD) patterns on the resultant phases indicated that each material was single phase and was in good agreement with the generated pattern from the single-crystal data (see the Supporting Information).

Characterization. Powder XRD patterns were collected on a SCINTAG XDS2000 diffractometer using Cu Kα radiation at room temperature with 35 kV and 30 mA to check the phase purity of the synthesized materials. Polycrystalline samples were mounted on glass sample holders and scanned in the 2θ range 5−70° with a step size of 0.02° and a step time of 1 s. TGA was performed on a Setaram LABSYS TG-DTA/DSC thermogravimetric analyzer. The polycrystalline samples were contained within alumina crucibles and heated at a rate of 10 °C min^{-1} from room temperature to 1000 °C under flowing argon. Scanning electron microscopy (SEM)/energy-dispersive analysis of X-rays (EDAX) were performed using a Hitachi S-3400N/Horiba Energy EX-250 instruments. EDAX for $Sb_2ZnO_3Cl_2$ and $Sb_{16}Cd_8O_{25}Cl_{14}$ reveals Sb:Zn:Cl and Sb:Cd:Cl ratios of approximately 2:1:2. IR spectra were recorded on a Varian 1000 FT-IR spectrometer in the 400−4000 cm^{-1} range, with the samples intimately pressed between two KBr pellets. IR for $Sb_2ZnO_3Cl_2$ (KBr, cm^{-1}): 871 (w), 834 (w), 793 (s), 712 (m), 643 (s), 562 (s), 543 (w), 526 (w). IR for $Sb_{16}Cd_8O_{25}Cl_{14}$ (KBr, cm^{-1}): 761 (w), 688 (s), 606 (s), 530 (w), 472 (w), 415 (w). Ion-exchange reactions were performed by stirring ca. 100 mg of a $Sb_{16}Cd_8O_{25}Cl_{14}$ sample in 3 mL of a 1 M aqueous solution of the following metal salts: NaF, KBr, and $NaNO_3$. The reactions were performed at room temperature and 150 °C for 24 h. The reaction products were recovered by filtration, washed with excess H_2O, and dried in air for 1 day.

Table 1. Crystallographic Data for $Sb_2ZnO_3Cl_2$ and $Sb_{16}Cd_8O_{25}Cl_{14}$

formula	$Sb_2ZnO_3Cl_2$	$Sb_2Cd_1O_{3.125}Cl_{1.75}$
fw	427.77	467.94
space group	*Pnma* (No. 62)	*I*2/*m* (No. 12)
a (Å)	17.124(4)	14.251(3)
b (Å)	5.5598(12)	3.9895(8)
c (Å)	6.4823(14)	21.145(4)
β (deg)	90	97.35(3)
V	617.2(2)	1192.3(4)
Z	4	8
T (°C)	298.0(2)	298.0(2)
λ (Å)	0.71073	0.70173
ρ_{calcd} (g cm^{-3})	4.604	5.214
μ (mm^{-1})	13.321	13.224
$R(F)^a$	0.0347	0.0470
$R_w(F_o^2)^b$	0.0886	0.1584

$^a R(F) = \sum||F_o| - |F_c||/\sum|F_o|$. $^b R_w(F_o^2) = [\sum w(F_o^2 - F_c^2)^2/\sum w(F_o^2)^2]^{1/2}$.

Single-Crystal XRD. The structures of $Sb_2ZnO_3Cl_2$ and $Sb_{16}Cd_8O_{25}Cl_{14}$ were determined by standard crystallographic methods. Colorless rod crystals of dimensions 0.04 × 0.08 × 0.25 mm^3 for $Sb_2ZnO_3Cl_2$ and 0.04 × 0.06 × 0.30 mm^3 for $Sb_{16}Cd_8O_{25}Cl_{14}$ were used for single-crystal XRD. The data were collected using a Bruker SMART APEX CCD X-ray diffractometer at the Korea Basic Science Institute at room temperature using graphite-monochromated Mo Kα radiation. A hemisphere of data was collected using a narrow-frame method with ω scan widths of 0.30°, and an exposure time of 5 s $frame^{-1}$. The first 50 frames were remeasured at the end of the data collection to monitor the instrument and crystal stability. The maximum correction applied to the intensities was < 1%. The data were integrated using the Bruker *SAINT* program,[30] with the intensities corrected for Lorentz, polarization, air absorption, and absorption attributable to the variation in the path length through the detector faceplate. A semiempirical absorption correction was made on the hemisphere of data with the *SADABS* program.[31] The data were solved and refined using *SHELXS-97* and *SHELXL-97*, respectively.[32,33] All of the atoms were refined with anisotropic displacement parameters and converged for $I > 2(I)$. All calculations were performed using the *WinGX-98* crystallographic software package.[34] Crystallographic data and selected bond distances for $Sb_2ZnO_3Cl_2$ and $Sb_{16}Cd_8O_{25}Cl_{14}$ are given in Tables 1 and 2. During the course of the refinement for $Sb_{16}Cd_8O_{25}Cl_{14}$, we determined that fractional occupancy must occur in O(5) and O(6) in order to maintain the charge balance. Also, much higher displacement parameters were observed if O(5) and O(6) are assumed to be fully occupied. For Sb(4), the bond distances to O(5) and O(6) are 2.46(3) and 2.362(15) Å, respectively. The distances are substantially longer than what is observed normally for Sb^{3+}−O bonds, indicating some partial occupancy in O(5) and O(6). Similarly, for Cd(1), the Cd(1)−O(5) bond distance [2.51(3) Å] is longer than other Cd^{2+}−O contacts, suggesting partial occupancy

(25) Mayerová, Z.; Johnsson, M.; Lidin, S. *Angew. Chem., Int. Ed.* **2006**, *45*, 5602.
(26) Pervukhina, N. V.; Borisov, S. V.; Magarill, S. A.; Naumov, D. Y.; Vasilev, V. I. *Am. Mineral.* **2008**, *93*, 1666.
(27) Thuillier-Chevin, F.; Maraine, P.; Perez, G. *Rev. Chim. Miner.* **1980**, *17*, 102.
(28) Sillen, L. G.; Melander, L. *Z. Kristallogr. Kristallgeom. Kristallphys. Kristallchem.* **1941**, *103*, 420.
(29) Alonso, J. A. *J. Chem. Soc., Dalton Trans.* **1998**, 1947.
(30) *SAINT, Program for Area Detector Absorption Correction*, version 4.05; Siemens Analytical X-ray Instruments: Madison, WI, **1995**.
(31) Blessing, R. H. *Acta Crystallogr.* **1995**, *A51*, 33.
(32) Sheldrick, G. M. *SHELXS-97—A program for automatic solution of crystal structures*; University of Goettingen: Goettingen, Germany, **1997**.
(33) Sheldrick, G. M. *SHELXL-97—A program for crystal structure refinement*; University of Goettingen: Goettingen, Germany, **1997**.
(34) Farrugia, L. J. *J. Appl. Crystallogr.* **1999**, *32*, 837.

Table 2. Selected Bond Distances (Å) for $Sb_2ZnO_3Cl_2$ and $Sb_{16}Cd_8O_{25}Cl_{14}$

		$Sb_2ZnO_3Cl_2$	
Sb(1)−O(1)	1.956(6)	Sb(1)−O(2) × 2	1.997(3)
Sb(2)−O(1)	1.936(6)	Sb(2)−O(2) × 2	2.017(3)
Zn(1)−O(2) × 2	2.069(3)	Zn(1)−Cl(1)	2.252(2)
Zn(1)−Cl(2)	2.244(2)		
		$Sb_{16}Cd_8O_{25}Cl_{14}$	
Sb(1)−O(1)	2.04(2)	Sb(1)−O(2) × 2	2.157(8)
Sb(1)−O(3)	1.98(2)	Sb(2)−O(1) × 2	2.174(9)
Sb(2)−O(2)	2.06(2)	Sb(2)−O(4)	1.983(19)
Sb(3)−O(4)	1.980(17)	Sb(3)−O(5) × 2	2.172(12)
Sb(3)−O(6)	1.99(3)	Sb(4)−O(3) × 2	2.499(11)
Sb(4)−O(5)	2.46(3)	Sb(4)−O(6) × 2	2.362(15)
Sb(4)−O(7)	1.963(15)	Cd(1)−O(3)	2.358(19)
Cd(1)−O(4) × 2	2.66(2)	Cd(1)−O(5)	2.51(3)
Cd(1)−O(7)	2.266(16)	Cd(1)−O(7) × 2	2.367(8)
Cd(2)−Cl(1)	2.661(5)	Cd(2)−Cl(1) × 2	2.731(4)
Cd(2)−Cl(2) × 2	2.633(4)	Cd(2)−Cl(3)	2.495(6)

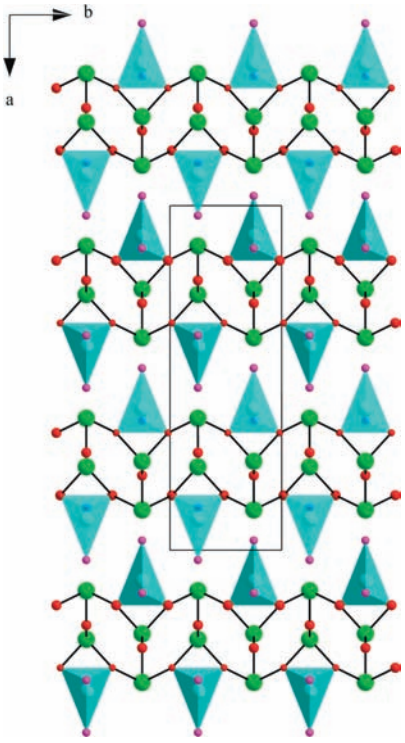

Figure 1. Ball-and-stick and polyhedral representation of $Sb_2ZnO_3Cl_2$. The distorted ZnO_2Cl_2 tetrahedra link to the $Sb^{3+}O_3$ layer on both sides, above and below along the [100] direction, and complete a layered structure of $Sb_2ZnO_3Cl_2$ (green, Sb; cyan, Zn; purple, Cl; red, O).

in O(5). In doing so, partial occupancies of 0.61(4) and 0.64(4) were refined for O(5) and O(6), respectively.

Results and Discussion

$Sb_2ZnO_3Cl_2$. $Sb_2ZnO_3Cl_2$ crystallizes in an orthorhombic space group *Pnma* (No. 62). The structure is composed of distorted ZnO_2Cl_2 tetrahedra and SbO_3 polyhedra that are connected through oxygen atoms (see Figure 1). The unique Zn^{2+} cation is connected to two oxygen and two chlorine atoms. The Zn−O and Zn−Cl bond distances are 2.069(3) and 2.244(2)−2.252(2) Å, respectively. The O−Zn−O, O−Zn−Cl, and Cl−Zn−Cl bond angles are 77.37(18)°, 106.73(11)−111.51(11)°, and 130.35(10)°, respectively. Two unique

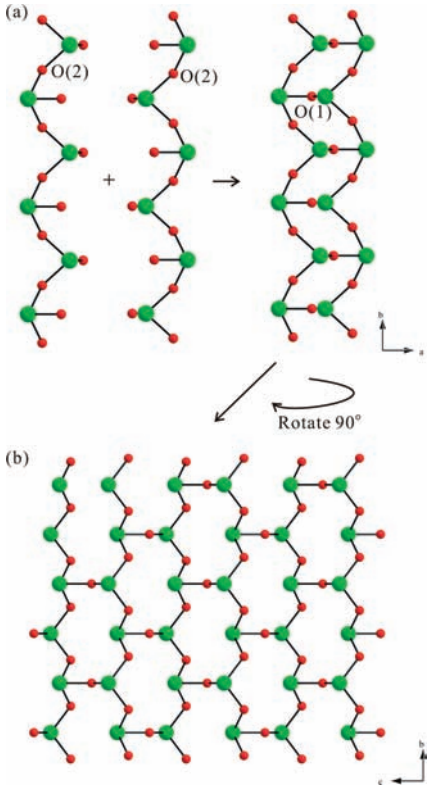

Figure 2. Ball-and-stick models representing the formation of (a) SbO_3 chains along the [010] direction and (b) a two-dimensional layer of SbO_3 polyhedra in the *bc* plane. Note: six-membered rings are observed in the layer (green, Sb; red, O).

Sb^{3+} cations are connected to three oxygen atoms and show a local asymmetric coordination environment in SbO_3 polyhedra attributable to the lone pairs. The Sb−O bond lengths range from 1.936(6) to 2.017(3) Å. The three-coordinate asymmetric $Sb(1)O_3$ and $Sb(2)O_3$ polyhedra are sharing their corners through O(2) along the [010] direction and are forming a unidimensional chain (see Figure 2a). The SbO_3 chains are further connected by O(1) along the [100] direction, which result in a corrugated two-dimensional layered structure (see Figure 2). Interestingly, six-membered rings composed of only SbO_3 polyhedra are observed in the layer. A similar layer topology has been observed for $SbTeO_3Cl$;[29] however, the $[SbTeO_3]^+$ layer in $SbTeO_3Cl$ consists of both TeO_3 and SbO_3 polyhedra. The dimensions of the six-membered rings are approximately 5.14 Å × 2.93 Å, taking into account the ionic radii of antimony.[35] The ZnO_2Cl_2 tetrahedra link to the $Sb^{3+}O_3$ layer on both sides, above and below along the [100] direction, and complete a layered structure of $Sb_2ZnO_3Cl_2$. In connectivity terms, $Sb_2ZnO_3Cl_2$ can be formulated as consisting of neutral layers of $\{2[Sb^{3+}O_{1/2}O_{2/3}]^{2/3+}[ZnO_{2/3}Cl_{2/1}]^{4/3-}\}^0$. Interestingly, the lone-pair cation Sb^{3+} contains an oxygen ligand only, and all of the chlorine atoms are coordinated to Zn^{2+}. Bond-valence calculations[36,37] resulted in values of 2.88−2.92 and 1.85 for Sb^{3+} and Zn^{2+}, respectively.

$Sb_{16}Cd_8O_{25}Cl_{14}$. $Sb_{16}Cd_8O_{25}Cl_{14}$ crystallizes in a monoclinic space group *I*2/*m* (No. 12). The structure of

(35) Shannon, R. D. *Acta Crystallogr.* **1976**, *A32*, 751.
(36) Brown, I. D.; Altermatt, D. *Acta Crystallogr.* **1985**, *B41*, 244.
(37) Brese, N. E.; O'Keeffe, M. *Acta Crystallogr.* **1991**, *B47*, 192.

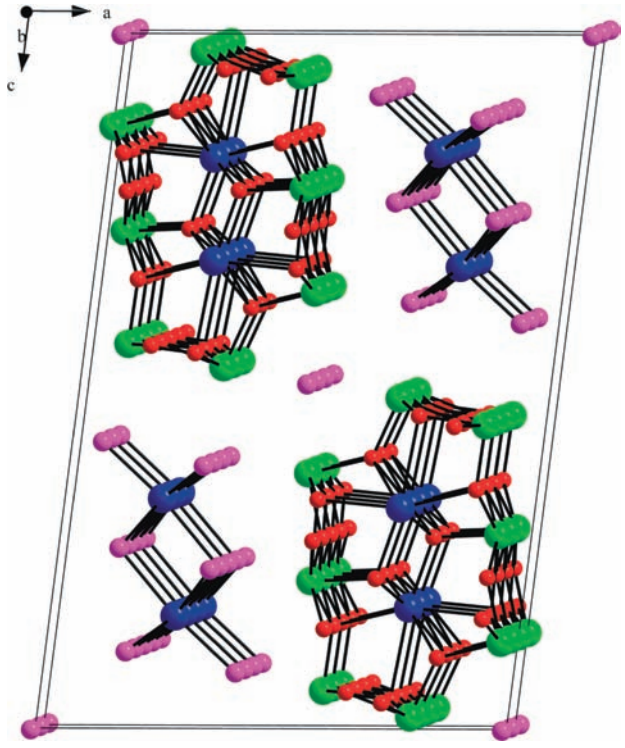

Figure 3. Ball-and-stick representation of $Sb_{16}Cd_8O_{25}Cl_{14}$ in the *ac* plane (green, Sb; blue, Cd; purple, Cl; red, O). Note: Sb^{3+}−Cd^{2+}−oxide rods, Cd^{2+}−chloride double chains, and isolated Cl^- ions are observed along the [010] direction.

$Sb_{16}Cd_8O_{25}Cl_{14}$ consists of Sb^{3+}−Cd^{2+}−oxide rods, Cd^{2+}−chloride double chains, and isolated Cl^- ions along the [010] direction (Figure 3). Within the Sb^{3+}−Cd^{2+}−oxide rods, most Sb^{3+} cations exhibit a SbO_4 "see-saw" environment, with the Sb−O bond distances ranging from 1.980(17) to 2.174(9) Å. The $Sb(4)^{3+}$ cation, however, reveals a SbO_6 group, with the Sb−O bond lengths ranging from 1.963(15) to 2.499(11) Å. In fact, O(5) and O(6) are partially occupied [0.61(4) and 0.64(4), respectively]; thus, the actual environment around the $Sb(4)^{3+}$ cation is the SbO_4 group. All of the Sb^{3+} cations are in a highly asymmetric coordination environment attributable to their nonbonded electron pair. The Sb^{3+}−O bond distances are consistent with those previously reported.[38] Within the Sb^{3+}−Cd^{2+}−oxide rods, the CdO_7 polyhedra are also observed, with the Cd−O bond lengths ranging from 2.266(16) to 2.66(2) Å. However, the connected oxygen atom O(5) is again partially occupied, indicating that the Cd−oxide moiety is, in fact, the CdO_6 group. The CdO_6 polyhedra share their edges through O(4) and O(7) and form a chain along the [010] direction. Each CdO_6 chain is further connected through O(7) along the [001] direction and forms a double chain along the [010] direction (see Figure 4a). On the other hand, the SbO_4 polyhedra share their oxygen ligands and produce an unprecedented one-dimensional tubular structure along the [010] direction (Figure 4b). Interestingly, the antimony oxide tube is wrapping the CdO_6 double chain through O(3), O(4), O(5), and O(7) and completes a unidimensional Sb^{3+}−Cd^{2+}−oxide rod (Figure 4c). Thus, all of the lone pairs in the Sb^{3+} cations are pointing outward around the rod. Infinite tubes consisting of $Sb^{3+}O_3$ and $Sb^{3+}O_4$ polyhedra were observed from $Sb_8O_{11}Cl_2$.[38] However, in $Sb_8O_{11}Cl_2$, the lone pairs point both inward and outward from the tubes. The Cd^{2+}−chloride double chains consist of $CdCl_6$ octahedra, with the Cd−Cl bond distances ranging from 2.495(6) to 2.731(4) Å. Similar to that of the CdO_6 double chain, each $CdCl_6$ octahedron shares its edges through Cl(1) and Cl(2) and forms a chain along the [010] direction. Each $CdCl_6$ chain is further linked through Cl(1) via edge-sharing along the [001] direction and produces an isolated double chain along the [010] direction (Figure 5). Similar isolated double chains have been observed for $[C_3H_7N_2S][CdCl_3]$[39] and $[Cd_2(Te_6O_{13})][Cd_2Cl_6]$.[40] The lone pairs associated with Sb^{3+} may be responsible for the separation of the structure. Because the Sb^{3+}−oxides with lone pairs wrap around the CdO_6 double chain, an enormous nonbonding tube with all of the lone pairs pointing outward was generated. On the other hand, the more halophilic metal cadmium forms separate chains of $CdCl_6$. This similar phenomenon has been observed in $CuSbTeO_3Cl_2$,[20] $CuSb_2O_3Br$,[21] and $Cu_{20}Sb_{35}O_{44}Cl_{37}$.[25] Finally, the isolated Cl^- anion is in an approximate cube environment, surrounded by eight Sb^{3+} cations at a distance of 3.360(11)−3.375(6) Å. The isolated Cl^- anion can be considered an "anionic template" in order to complete a stable crystal structure. An anionic template effect similar to that of Cl^- anion has been observed from the three-dimensional $Te_4Nb_3O_{15}\cdot Cl$.[41] Bond-valence calculations[36,37] on $Sb_{16}Cd_8O_{25}Cl_{14}$ resulted in values of 2.93−3.10 and 1.82−1.99 for Sb^{3+} and Cd^{2+}, respectively.

IR Spectroscopy. The IR spectra of $Sb_2ZnO_3Cl_2$ and $Sb_{16}Cd_8O_{25}Cl_{14}$ reveal characteristic Sb−O vibrations in the region of about 606−871 cm^{-1}. Characteristic IR bands for Zn−O vibrations are observed around 520−562 cm^{-1}. Stretches centered at 415 and 472 cm^{-1} can be assigned to Cd−O vibrations. The assignments are consistent with those previously reported.[42]

TGA. The thermal behaviors of $Sb_2ZnO_3Cl_2$ and $Sb_{16}Cd_8O_{25}Cl_{14}$ were investigated using TGA. TGA of both materials under flowing argon indicates that $Sb_2ZnO_3Cl_2$ and $Sb_{16}Cd_8O_{25}Cl_{14}$ are robust with decomposition temperatures of 460 and 650 °C, respectively. Above those temperatures, the materials started to decompose, which may be attributable to the loss of chlorine atoms. Thermal decomposition products at 1000 °C in air for $Sb_2ZnO_3Cl_2$ and $Sb_{16}Cd_8O_{25}Cl_{14}$ resulted in $ZnSb_2O_6$[43] and Sb_6O_{13},[44] respectively, with some unknown mixture as shown by powder XRD measurements. The TGA data have been deposited in the Supporting Information.

Ion-Exchange Reactions. The structural topology of $Sb_{16}Cd_8O_{25}Cl_{14}$ suggested that the material may be able to undertake ion-exchange reactions in which the isolated

(38) Mayerová, Z.; Johnsson, M.; Lidin, S. *Solid State Sci.* **2006**, *8*, 849.
(39) Kubiak, M.; Glowiak, T.; Kozlowski, H. *Acta Crystallogr.* **1983**, *C39*, 1637.
(40) Jiang, H.-L.; Mao, J.-G. *Inorg. Chem.* **2006**, *45*, 717.
(41) Ok, K. M.; Halasyamani, P. S. *Inorg. Chem.* **2002**, *41*, 3805.
(42) Nakamoto, K. *Infrared and Raman Spectra of Inorganic and Coordination Compounds*; Wiley: New York, 1997.
(43) Stahl, S. *Ark. Kemi, Mineral. Geol.* **1943**, *17B*, 1.
(44) Dehlinger, U.; Glocker, R. *Z. Anorg. Allg. Chem.* **1927**, *165*, 41.

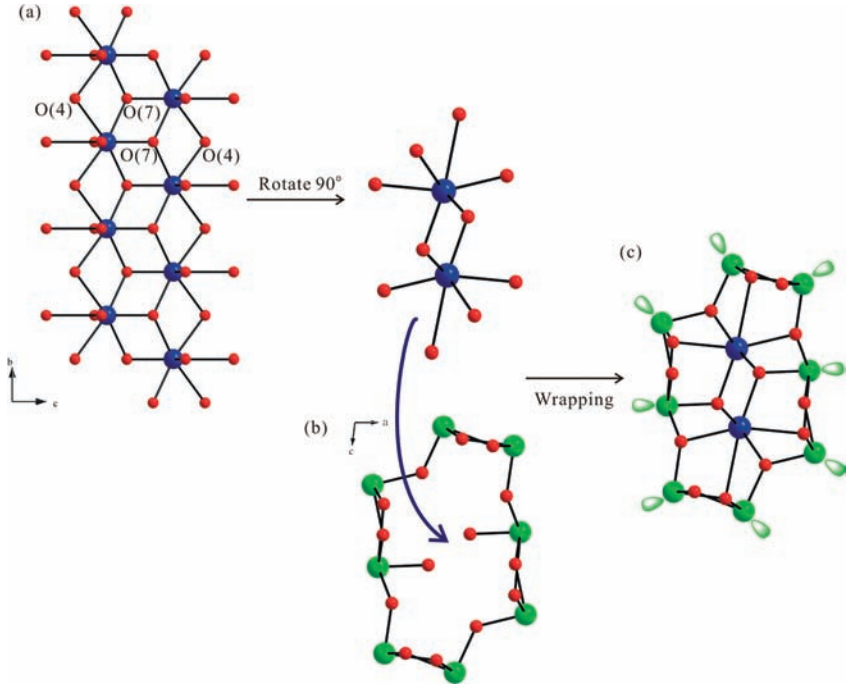

Figure 4. Ball-and-stick models representing how the $Sb^{3+}-Cd^{2+}-$oxide rod is generated in $Sb_{16}Cd_8O_{25}Cl_{14}$ (green, Sb; blue, Cd; red, O). (a) Edge-sharing CdO_6 chains are further connected through O(7) to form a double chain along the [010] direction. (b) SbO_4 polyhedra share their oxygen ligands and produce an interesting one-dimensional tubular structure along the [010] direction. (c) Antimony oxide tube wrapping the CdO_6 double chain and completing a unidimensional $Sb^{3+}-Cd^{2+}-$oxide rod. Note: all of the lone pairs in the Sb^{3+} cations are pointing outward around the rod.

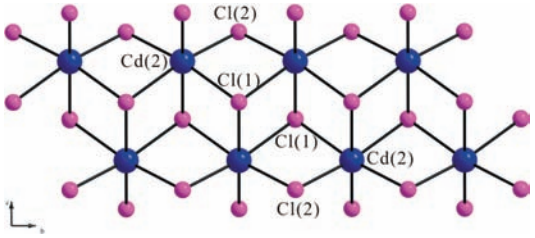

Figure 5. Ball-and-stick models representing a one-dimensional double chain of $CdCl_6$ in $Sb_{16}Cd_8O_{25}Cl_{14}$ along the [010] direction (blue, Cd; purple, Cl).

Cl^- anion is replaced by other anions. Initially, approximately 100 mg of $Sb_{16}Cd_8O_{25}Cl_{14}$ was stirred in 3 mL of 1 M solutions of NaF, KBr, and $NaNO_3$ for 1 day at room temperature. The ion-exchange experiments indicated that exchanging Cl^- for other anions is difficult under mild conditions. It is not difficult to understand why no ion-exchange behavior is observed when we examine the structure more closely. As can be seen in Figure 6, all of the lone pairs point above and below the chloride so that the chloride anions are effectively locked in place, which prevents any mobility for the anion. Further attempts have been made to exchange the Cl^- anions at 150 °C for 24 h. The powder XRD analyses on the recovered products, however, revealed that the materials decomposed to Sb_2O_3 and some unknown mixture.

Dipole Moment Calculations. Both $Sb_2ZnO_3Cl_2$ and $Sb_{16}Cd_8O_{25}Cl_{14}$ contain a cation in an asymmetric coordination environment, i.e., Sb^{3+}. One of our motivations for investigating materials containing asymmetric lone-pair cations is to better understand these coordination environments, although they crystallize in centrosymmetric space groups. The direction and magnitude of the distortions in

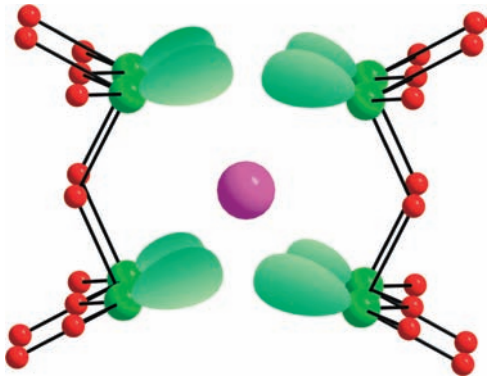

Figure 6. Ball-and-stick diagram representing how the Sb^{3+} lone pairs (shown schematically) in $Sb_{16}Cd_8O_{25}Cl_{14}$ impede the movement of the Cl^- anion.

the SbO_x ($x = 3-5$) polyhedra may be quantified by determining their local dipole moments. This approach has been described earlier, where a bond-valence calculation was used to calculate the direction and magnitude of the local dipole moments.[45−47] With the polyhedra containing lone pairs, the lone pair is given a charge of 2− and the localized $Sb^{3+}-$lone pair distance is estimated to be 1.08 Å based on the work of Galy and Meunier.[48] Using this methodology, the dipole moment for the SbO_x polyhedra is in the opposite direction of the lone pair. We have calculated the dipole moment of the SbO_x polyhedra in $Sb_2ZnO_3Cl_2$ and $Sb_{16}Cd_8O_{25}Cl_{14}$. For comparison, we

(45) Maggard, P. A.; Nault, T. S.; Stern, C. L.; Poeppelmeier, K. R. *J. Solid State Chem.* **2003**, *175*, 27.
(46) Izumi, H. K.; Kirsch, J. E.; Stern, C. L.; Poeppelmeier, K. R. *Inorg. Chem.* **2005**, *44*, 884.
(47) Ok, K. M.; Halasyamani, P. S. *Inorg. Chem.* **2005**, *44*, 9353.
(48) Galy, J.; Meunier, G. *J. Solid State Chem.* **1975**, *13*, 142.

Table 3. Summary of the Dipole Moments for SbO_x ($x = 3-5$) Polyhedra (D = Debye)

SbO_x		dipole moment (D)
SbO_3 (48 examples)	range	4.35−9.64
	average	7.55
SbO_4 (51 examples)	range	3.79−11.29
	average	8.35
SbO_5 (7 examples)	range	6.22−9.80
	average	7.68

have also calculated the dipole moment for similar polyhedra in other Sb^{3+}−oxides as well as Sb^{3+}−oxyhalides (see Table 3). As is seen in Table 3, the magnitude of the SbO_x dipole moments shows only a small difference. In fact, an examination of 48 examples of SbO_3 polyhedra reveals that the dipole moments range from 4.35 to 9.64 D and have an average value of 7.55 D. Similarly, 51 examples of SbO_4 exhibit dipole moments ranging from 3.79 to 11.29 D, with an average value of 8.35 D. Although not as many examples have been reported, 7 examples of SbO_5 polyhedra resulted in an average dipole moment of 7.68 D. A complete discussion of the dipole moment calculations on the SbO_x polyhedra will be reported shortly.

Conclusions

We have successfully synthesized the first examples of antimony/zinc oxychloride, $Sb_2ZnO_3Cl_2$, and antimony/cadmium oxychloride, $Sb_{16}Cd_8O_{25}Cl_{14}$, through standard solid-state reactions. The materials were characterized by single-crystal and powder XRD as well as IR spectra, TGA, ion-exchange reactions, and dipole moment calculations. Both materials contain asymmetric lone-pair cation Sb^{3+} in the structures. $Sb_2ZnO_3Cl_2$ has a novel two-dimensional layered structure consisting of distorted ZnO_2Cl_2 tetrahedra and SbO_3 polyhedra. $Sb_{16}Cd_8O_{25}Cl_{14}$ exhibits a one-dimensional structure consisting of $Sb^{3+}-Cd^{2+}$−oxide rods, Cd^{2+}−chloride double chains, and anionic template Cl^- ions. We continue to explore the synthesis of new Sb^{3+}−oxychlorides as well as investigate the incorporation of other cations with stereoactive lone pairs into new materials.

Acknowledgment. This research was supported by Nuclear Research & Development Program of the National Research Foundation of Korea (NRF) funded by the Ministry of Education, Science & Technology (MEST) (Grant 2009-0083266).

Supporting Information Available: X-ray crystallographic files for $Sb_2ZnO_3Cl_2$ and $Sb_{16}Cd_8O_{25}Cl_{14}$ in CIF format, experimental and calculated powder XRD patterns, TGA diagrams, and IR spectra. This material is available free of charge via the Internet at http://pubs.acs.org.